Accepted Manuscript

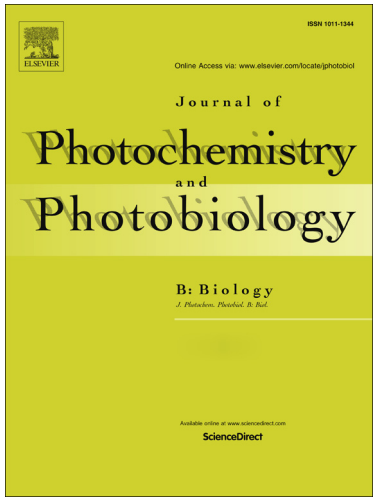

Nonadiabatic tapered optical fiber sensor for measurement of antimicrobial activity of silver nanoparticles against *Escherichia coli*

Mohammad Ismail Zibaii, Hamid Latifi, Zahra Saeedian, Zinab Chenari

PII: S1011-1344(14)00091-8
DOI: http://dx.doi.org/10.1016/j.jphotobiol.2014.03.017
Reference: JPB 9700

To appear in: *Journal of Photochemistry and Photobiology B: Biology*

Received Date: 7 December 2013
Revised Date: 17 February 2014
Accepted Date: 18 March 2014

Please cite this article as: M.I. Zibaii, H. Latifi, Z. Saeedian, Z. Chenari, Nonadiabatic tapered optical fiber sensor for measurement of antimicrobial activity of silver nanoparticles against *Escherichia coli*, *Journal of Photochemistry and Photobiology B: Biology* (2014), doi: http://dx.doi.org/10.1016/j.jphotobiol.2014.03.017

Nonadiabatic tapered optical fiber sensor for measurement of antimicrobial activity of silver nanoparticles against *Escherichia coli*

Mohammad Ismail Zibaii[a], Hamid Latifi[a*], Zahra Saeedian[a], Zinab Chenari[a]

[*]Corresponding author.Tel.982129904254; fax: 22431775. E-mail address: Latifi@ sbu.ac.ir

(H.Latifi)

[a]Laser & Plasma Research Institute, Shahid Beheshti University, Evin, Tehran, Iran.

Abstract

Silver nanoparticles (SNPs) exhibit antibacterial properties via bacterial inactivation and growth inhibition but the mechanism is not yet completely understood. In this study a label free and rapid detection method for study of antimicrobial activity of the SNP against *Escherichia coli* (*E.coli K-12*) is investigated using a nonadiabtic tapered fiber optic (NATOF) biosensor. The results show that SNPs interact with bacteria either by anchoring to or penetrating into the bacterial cell layer. These mechanism changes the refractive index (RI) of the tapered region, which in turn lead to the changes in the optical characteristics of the tapered fiber and output signals. With similar conditions for bacteria, the inhibition rate of the *E. coli* growth was measured by colony counting method as an experimental control and the results were compared with those obtained from the fiber sensor measurements. For SNP concentrations ranging from 0 to 50 μg ml^{-1} the inhibition rates of the *E. coli* growth were measured to be from 1.27 h^{-1} to - 0.69 h^{-1} and from – 3.00×10^{-3} h^{-1} to - 1.98×10^{-2} h^{-1} for colony counting and optical fiber biosensor, respectively. The results demonstrate the potential of the proposed NATOF biosensor as a label free and rapid sensing platform for understanding the mechanism of antibacterial effects of SNPs.

Keywords: silver nanoparticle; nonadiabatic tapered optical fiber; *E.coli,* refractive index; biosensor and inhibition rate.

1- Introduction

Silver nanoparticles (SNPs) display unique, superior and indispensable properties and have attracted much attention for their distinct physical and chemical characteristics. Their uniqueness arises specifically from higher surface to volume ratio, modified structure, controlled surface composition and reactivity. They represent an important material in the development of novel devices that can be used in various physical, biological, biomedical and pharmaceutical applications [1-4].

The SNPs has attracted attention as an alternative antibacterial agent for common application in consumer products [5-9]. Such compounds can reduce infections in burns patients and prevent bacterial colonization of prostheses, catheters, dental materials and human skin [10-14]. Recent studies have focused on different aspects of the physicochemical properties of SNPs, responsible for the inhibitory effect on microorganisms. It has been shown that the SNPs inactivate of *E. coli* which depends concentration of these particles [4,6,15], as well as bacterial type [6, 8], presence of Ag (I) [6], SNP shape [8], and size [2,6,9].

There are several methods to investigate the interaction between bacteria and SNPs including optical density measurement (OD) [16], colony counting [17], scanning electron microscopy (SEM) [6], transmission electron microscopy (TEM) [2,6], X-ray energy dispersive spectrometry (XEDS) [2,6], *Kirby-Bauer* diffusion [18] and Atomic Force Microscopy (AFM) analysis [19]. These methods are summarized and compared in Table 1 using minimum inhibitory concentrations (MICs).

[Table 1 should be inserted in here]

Over the past decade, biosensor technology has been intensively studied as a sensitive and reliable detection tool that enable researchers to obtain data instantaneously for detection of a specific analyte in a minimum amount of time and preparation steps, compared to conventional methods [20-22]. Fiber-optic biosensors are one of the most widely studied for rapid detection of many pathogens, toxins, proteins, and hormones [23]. Several techniques for fluorescence-based detection of *E. coli* have been proposed in

recent past years including optical waveguide comprised of glass capillary [24], polystyrene waveguide [25] and uniform MM polystyrene [26,27]. Currently, Label-free method is a new and powerful way of determining the growth rate of living cells. These methods rely on the changes which occur at the sensor surface that in turn could modify the optical properties of a sensor, such as changes in the analyte RI or changes in the thickness of biofilm. Among these techniques, fiber optic biosensors based on RI sensing rely exclusively on optical transduction mechanisms for detecting target biomolecules.

Furthermore, several different structures such as tapered optical fibers [28-30], chemical etched optical fiber [31], U-bent optical fiber [32], Surface Plasmon Resonance (SPR) [33-38], micro-optical resonators [39,40], long period fiber grating [41-42], and THz photonic crystal fiber [43] have been proposed for *E. coli* detection. The biosensing applications to date the target detected, matrix, the limit of detection (LOD), sensor geometry, fiber type, principles of detection and references are summarized in Table 2.

In this paper, a label free method is used to measure inhibition rate in the *E. coli K-12* growth with a nonadiabatic tapered optical fiber (NATOF) biosensor at room temperature. This new sensing method for measurement of the inhibition of the bacterial growth displays a fast response and high sensitivity. These characteristics give them preference over other techniques for biological applications. In our pervious study we measured bacterial growth rate of *E. coli k-12* by NATOF bioseonsor which LOD equal to 60 bacteria mm^{-2} [30]. To our best knowledge, while the antibacterial activity of SNP is well known and has been studied in detail [2,6,9], the antibacterial activity of SNP with fiber optic biosensor has not ever been reported in the literature.

[Table 2 should be inserted in here]

2. Principle of nonadiabatic tapered optical fiber

The penetration depth of the evanescent field (EVF) in a normal single mode fiber is much smaller than the cladding thickness. For fiber optic biosensor applications, we need to increase the magnitude and the penetration depth of the EVF which can be enhanced significantly by tapering.

The NATOFs can be fabricated in such a way that coupling occurs primarily between the fundamental core mode LP_{01}^{core} of the un-pulled fiber and the fundamental cladding mode of LP_{01}^{clad} and high-order cladding modes of LP_{0m}^{clad} [23,44-45]. The multiple cladding modes are excited by the down-taper region continuously propagate through the central uniform waist region and are coupled back into the fiber core via the up-taper region to form a modal Mach–Zehnder interferometer (MFMZI). Fig. 1 shows a conceptual scheme of the sensing probe (a) and its behavior as a two waves interferometer (b).

[Figure 1 should be inserted in here]

The phase difference ΔΦ between the LP_{01}^{clad} mode and LP_{0m}^{clad} modes can be expressed as $\Delta\Phi=2\pi\Delta n_{eff}^{m}L/\lambda$, where Δn_{eff}^{m} is the difference in the effective RI between the fundamental cladding mode and m-th cladding mode LP_{0m}^{clad}, λ is the operation wavelength, and L is the interference length [46-47]. Therefore, the spectral response of the taper will shift correspondingly by changing the above terms.

In intensity measurement, understanding the loss in NATOF is important. When higher-order modes reach to the single mode region, they cannot be guided by the fiber anymore, and are diffract out as radiative modes. In addition, when the RI in the environment is higher than clad, the mode is lost in to the environment by scattering and absorption [28, 48-49]. In this study, with the growth or inhibition of the bacteria on the tapered region, changes in the RI of the clad leads to changes in optical throughput [23,46–47]. By measuring changes of the transmitted light the related bacterial surface concentration can be determined.

3. Materials and Methods

3-1 Material

Escherchia coli strain *K-12* was used in this experiment purchased from the Iranian Research Organization for Science and Technology (IROST, Iran). In all procedures, Milli-Q HPLC grade water was used. The components of the Nutrient Broth (NB), Casein-peptone Soymeal-peptone Agar (CASO

Agar), yeast extract, and glucose medium used in growing and maintaining the bacteria cultures were purchased from Merck. Poly-l-lysine (PLL) was obtained from Aldrich Chemicals. SPNs were obtained from Medicinal Plants and Drugs Research Institute (Tehran, Iran) which the average particle size was 17 nm [50].

3-2 Experimental set up

The NATOF is fabricated by heat pulling method, using a CO_2 laser [2]. Schematic Experimental setup is shown in Fig. 2. The light source is edge light emitted diode (ELED) with the central wavelength, FWHM, and the power of 1547 nm, 79.6 nm, and 50 µw, respectively. After passing a dual stage isolator, the light of ELED arrives at the NATOF sensor. Spectral response of the NATOF was observed with an optical spectrum analyzer (OSA) (Agilent 86142B) having an accuracy, reproducibility of the wavelength, sensitivity and stability of amplitude equal to 10 pm, ±0.2 pm, ±0.01 dB and −60 dBm, respectively. The data from OSA was recorded by a GPIB interface on a computer. The recorded data were processed by a program code in the Labview software. Typical taper waist diameters, taper lengths, loss and free spectral range (FSR) were in the range of 6-8 µm, 17-20 mm, 9% and 7-10 nm, respectively. SEM microphotograph of one conic section of the NATOF is shown in Fig. 3.

[Figure 2 should be inserted in here]

[Figure 3 should be inserted in here]

3.3. Bacteria and culture method

E. coli K-12 were cultured in NB medium (NBM) until mid-exponential phase (14-18 h) and then centrifuged (Sigma, 3k30, 845 g, 5 min, 4 ^{0}C) to remove the supernatant. The pellet was resuspended in sterile phosphate-buffered saline-A (PBS-A) to obtain an *E. coli* concentration of approximately 10^8 colony-forming units (CFU) ml^{-1} as determined by 0.5 McFarland standard and spectrophotometric assays. Typical growth experiment was conducted by two growth mediums, NBM which contained colour

from the ingredients and inoculating non-colored glucose culture medium (GCM) (PBS-A, yeast extract (0.1 g l^{-1}) and glucose (1 g l^{-1})). The equal numbers of *E.coli* bacteria (10^8 CFU ml^{-1}) were used inoculate both growth mediums.

3.4. Pour plate method for inhibitory rate measurement

To examine the anti-bacterial effect of the SNPs on Gram-negative bacteria, approximately 10^8 CFU of *E. coli* were cultured for 60 min on GCM and NBM which supplemented with different concentrations of SNPs. Followed by sedimentation and re-culturing them in silver-free CASO Agar pleats. Control bacteria were treated similarly, however with no exposure to the SNPs. Growth rate was determined by colony counting method. First, 1 ml of the bacterial solution was added to the 250 ml of each growth mediums, which is labeled as sample flask. Using a sterile pipette tip, 0.1 ml of sample flask was removed every 30 min to prepare low concentration of bacterial solutions. Next, 0.1 ml of each serial dilution was transferred to appropriate CASO Agar plates. Plates were then incubated for 24 h at 37°C and the numbers of colonies were counted. The average counts on the three separate plates corresponding to a particular sample were calculated. In order to increase the accuracy of the counting, only the plates with 10 – 30 colonies were considered for calculation. Silver-free CASO Agar plates were cultured under the same conditions and were used as control.

3.5. Immobilization of tapered fiber

In the experimental setup, the NATOF was fixed under tension in the Plexiglass fiber holder preventing its bending inside the fiber holder. As a result strain was a constant parameter during the experiment and kept the tapered fiber in contact with liquid materials. To immobilize *E. coli* on the sensing area, the tapered section of each fiber was washed with 70% ethanol (v/v) containing 1% HCl (v/v), then rinsed with deionized water at room temperature. The fiber was then dried in microbiological safety cabinet for thirty minutes. Each taper fiber was overwhelmed by PLL solution of 0.1 % PLL and allowed to evaporate over night. *E. coli* (10^8 CFU ml^{-1}) suspended in sterile PBS-A and contacted with the taper for 30 min. Fibers were then rinsed twice gently in PBS-A to remove unattached bacteria.

3-6 Inhibition rate measurement with NATOF sensor

To examine the bacterial growth rate and to determine the growth curve in the presence of SNPs by optical fiber sensor, after the immobilization of *E. coli* on the NATOF surface, 100 cm^3 of GCM supplemented with SNPs at concentrations of 10, 20, 30 or 50 μg ml^{-1} was added into the fiber holder. Inhibition rates of the bacterial growth were determined by measuring the transmitted intensity of the NATOF for several hours.

4 Result and discussion

4.1. Analysis of antibacterial activity of SNPs in different growth mediums with colony counting method

The inhibition rate of the bacterial growth for the bacterial species is represented by the Eq. (1) [30, 51]:

$$\ln N=\ln N_0+\mu t \qquad (1)$$

where N is the bacterial cell count at the time t, N_0 is the initial cell count and μ is the inhibition growth rate constant. The experimental data were plotted in the logarithmic scale and derived the values of μ and $\ln N_0$ corresponding to different doses of the nanoparticles (x). Linear relationships of μ and $\ln N_0$ with x were derived as shown in Eq. (2), (3):

$$\mu=- a x+b \qquad (2)$$

$$\ln N_0=- c x-d \qquad (3)$$

Thus, Eq. (1) can be rewritten by replacing the values of μ and $\ln N_0$, as:

$$\ln N=(b t-d)-(a t+c) x \qquad (4)$$

Eq. (4) represents the inhibition rate of the bacterial growth in the presence of various concentrations of SNP in the medium.

In this study the influence of the bacterial media on the antibacterial effectiveness of the SNPs was examined. To analyse the antibacterial activity of SNPs in different growth mediums, *E. coli* were cultured on NBM and GCM supplemented with 0, 10, 20, 30, and 50 μg ml^{-1} of SNPs and the inhibition rate was measured with colony counting method as described in Section 3.4. Fig. 4 shows a typical image of different plates that are used to measure inhibition rate of the bacterial growth in NBM and GCM at 0, 10, 30 μg ml^{-1} concentration of SNP.

[Figure 4 should be inserted in here]

Plot of natural log of bacterial cell number ratio versus time for bacterial growth in NBM is shown in Fig. 5a. The calibration curves obtained for the first three hours allowed the estimation of correlation coefficients (R^2) equal to 0.996 and 0.976 and growth rate of 1.39 h^{-1} and 1.06 h^{-1} for 0 and 10 μg ml^{-1} of SNPs, respectively. Comparing the growth rate in 0 μg ml^{-1} with 10 μg ml^{-1} of SNPs, 24% inhibition in bacterial cell growth was observed. The results show that the growth rate after three hours equals to 1.87 h^{-1}, 1.61 h^{-1}, 1.80 h^{-1}, and 1.61 h^{-1} for 0, 10, 30 and 50 μg ml^{-1}, respectively. As the SNPs concentration increased, a delay in *E. coli* growth was observed for all cases. The lag phase was two hours and three hours for 30 μg ml^{-1} and 50 μg ml^{-1} of SNPs, respectively. It is observed that different concentrations of the SNPs have a less significant effect on the growth of bacteria in NBM. The concentration of the SNPs gradually decreases, allowing resumed growth of bacterial cells. This process is governed by the interaction of these particles with intracellular substances of the destroyed bacterial cells, causing SNPs coagulation and removal from the liquid system [6]. Obviously, these particles have only a limited use as biocidal materials in liquid systems because of their low colloidal stability. Also, NBM is a nutritious cultivation medium that allows bacterial exponential growth and as a result overcomes the amount of the bacterial destruction due to the interaction with SNPs.

Similar experiments were carried out using GCM. Results are demonstrated in Fig. 5b which show that the *E.coli* bacteria started to grow at t = 0 and C= 0 μg ml^{-1} in NBM culture medium, however, for GCM medium the growth began one hours after inoculation with a 0.7 slope ratio. Also, Fig. 5b shows that the

GCM containing 10 μg ml^{-1} of SNP growth rate is 63% lower than in NBM. This growth is also seen in C= 20 μg ml^{-1} and higher concentrations in which the bacterial degradation overcomes.

The inhibition rates of the bacterial growth in the GCM containing 10, 20, 30, and 50 μg ml^{-1} of SNP concentrations from 2 to 5 h were calculated to be 1.270 h^{-1}, 0.594 h^{-1}, -0.216 h^{-1}, -0.384 h^{-1} and -0.694 for 0, 10, 20, 30, and 50 μg ml^{-1}, respectively. For 10 μg ml^{-1} of SNP concentration compared to 0 μg ml^{-1} the growth rate decreased 53%. The concentration of 50 μg ml^{-1} is found to be strongly inhibitory effect for the growth of bacteria, as it takes about 8 h to initiate any noticeable growth. Therefore, using GCM is more suitable than NBM for testing the effect of different concentrations of SNPs in bacterial growth inhibition.

[Figure 5 should be inserted in here]

Fig. 6a shows a plot of inhibition rate of the bacterial growth versus concentration of the SNPs. A correlation coefficient (R^2) of 90%, and sensitivity of – 0.024 ml μg^{-1} s^{-1} was obtained by linear fitting. Plotting natural log of the initial bacterial cell versus concentration of the SNPs in Fig. 6b the linearity had a correlation coefficient (R^2) of 99%, and its sensitivity was – 0.038 cell ml μg^{-1} using a linear fit. The slope of linear fitting and intercept in Figs. 6a-6b can be used to obtain constant parameters in Eqs. (2) and (3). The obtained empirical coefficients as presented in Table 3 represent the dynamic growth rate of bacteria in the presence of different concentrations of SNPs in the GCM as a growth medium.

[Figure 6 should be inserted in here]

[Table 3 should be inserted in here]

4.2. Inhibition rate of the bacterial growth measurement by NATOF biosensor

To measure growth rate by optical fiber sensor the output power of a tapered fiber can be written as:

$$I=\alpha N^{\beta} \quad (5)$$

where N is the surface concentration per unit area, and α and β depend on the taper characteristics, as well as, optical properties of the *E. coli* which is grown on the taper. During the exponential growth phase bacterial culture media mimics a first-order chemical reaction, i.e. the rate of increase of the cells is proportional to the number of existing bacteria. The constant of proportionality, is an index of the growth rate that can be determined from Eq. (1).

With changing of RI with time due to bacterial growth, the output intensity through the tapered fiber also changes with time. In this case, the following analysis is valid as long as the time lag is constant; From Eq. (1) and Eq. (2), one can obtain:

$$\ln (I/I_0)=\beta \ln (N/N_0) \quad (6)$$

where, I_0 is the output power at the initial time. For a constant growth rate, Eq. (6) can be written as:

$$\ln (I/I_0)=\beta \mu t \quad (7)$$

Eq. (7) points out that the plot of ln (I/I_0) versus time will propose a straight line with the slope proportional to specific inhibition growth rate.

For measuring the inhibition in growth rate with NATOF sensor, first we measured output spectrum of the fiber sensor when it surrounded with the GCM containing SNPs for 2 h. During the tests the temperature of the solution was kept approximately constant (at room temperature) showing changes smaller than ± 0.5 °C. These fluctuations lead to wavelength shifts of about ± 0.01 nm, which is the OSA maximum accuracy. Therefore, during the test, the fixed NATOF on the fiber holder showed no cross sensitivity to temperature and strain. After recording the background spectrum, the sensor was rinsed with of PBS-A solution for several times and the bacteria were immobilized on the surface of sensor as described in Section 3.5.

Typical spectral response of the NATOF for before and after cell immobilization on the fiber is demonstrated in Fig. 7. With bacterial cell immobilizing on the tapered fiber considerable changes in

wavelength of the output spectrum is observed. Therefore measuring wavelength shift can be used for controlling of cell immobilizing procedure.

[Figure 7 should be inserted in here]

For measurement of the inhibition rate of the bacteria in GCM with different concentration of SNPs, different concentration of SNPs were added to the fiber sensor holder and data was recorded for 3 h. The interaction of bacteria with SNPs on the tapered fiber leads to changes in the optical characteristics of the tapered fiber. This affects the evanescent field leading to changes in optical throughput. The transmission output of the NATOF sensor can be used for measuring antibacterial activity. Obtained results are shown in Fig. 8.

[Figure 8 should be inserted in here]

Fig. 8a shows that the output of the sensor is reduced while the concentrations of the SNPs are increased in the culture medium. With linear fitting inhibition rate was calculated to be -3.00×10^{-3}, -3.12×10^{-3}, -1.71×10^{-2}, -1.98×10^{-2} for 0, 10, 20 and 50 μg ml^{-1} concentration of SNPs. The negative slope in Fig. 8b for SNP concentration in range 10, 20 and 50 μg ml^{-1} was 1.04, 5.7 and 6.6 times lower than the slope of 0 μg ml^{-1}. Also, these antibacterial activities of SNPs with the NATOF biosensor have been successfully detected and quantified in 3 h duration. The average time required to obtain information about the inhibition rate of SNPs is about 72 min. The NATOF biosensor is faster than conventional bacteriological techniques which can take 6-18 h. The inhibition rate of the bacterial growth calculated with colony counting method and fiber optic biosensor are shown in Table 4. The value of β can be determined from the Table 4 with measured growth rate by colony counting method and NATOF sensor in growth media without SNP which is found to be 2.4×10^{-3}.

[Table 4 should be inserted in here]

The optical attenuation observed for control experiment in GCM without SNP in Fig.8a could be generated by variation of the cladding refractive index and/or its thickness. When the bacteria are allowed

to grow around the NATOF biosensor, two effects can occur. As the bacteria start to grow the enzymes are released due to the bacteria metabolism resulting in the change of the RI [31]. Due to the existence of an increasing number of bacteria in contact with the fiber during the log phase, the medium becomes more opaque with time. Consequently the RI around the tapered surface also changes [30-31].

The dielectric constant of the biological medium is described by [30,40]:

$$\varepsilon(r)=\varepsilon_{background}+\delta\varepsilon \qquad (8)$$

where $\varepsilon_{background}$ is the dielectric constant of the background medium and δε indicates the variation of ε caused by the inhibition of the bacterial growth. For a typical bacteria cell, let n_w and n_p be the RIs of the cell wall and protoplasm, respectively. Then it can be shown that [30,40]:

$$\delta\varepsilon=\sigma[(n^2_w-n^2_{sol})A+(n^2_p-n^2_w)A'] \qquad (9)$$

where A (A_0) is the average projection cross sectional area of the outer (inner) surfaces of the cell on the tapered surface and σ is the average surface density of the cells. The cell wall thickness is estimated at a-a′ =b-b′ = 42 nm, RI of the bacteria cell wall (n_w=1.42), and protoplasm of the bacteria (n_p= 1.355), which results in the average refractive index of n≈1.37 associated with *E. coli* and n_{sol}=1.33 of the surrounding aqueous solution [37,51-52]. The presented RIs are associated with a λ = 1.311 μm central wavelength. The effective footprint of cylindrical area projection was found to be 2a×2b = 2 μm× 0.8 μm. σ is determined by counting the number of bacteria identified in the projected surface of 10.71 μm× 7.94 μm, which is only a fraction of the total taper surface. At the beginning of the experiment, the average surface density of the bacteria is about 2.35×10^{-2} *E. coli* μm^{-2}, which corresponds to an area occupied by approximately 2 bacteria. According to Eq. (9), the change in RI was observed to be about 1.4×10^{-3} RIU immediately after immobilizing *E. coli* on the taper. After initial immobilization, the growth of *E. coli* lying on the taper surface results in an average increase in the surface density of the cells and consequently an increase in the RI value of the taper cladding [30,31].

As can be seen in Fig.8b the output intensity of the NATOF biosensor is decreased with interacting SNPs with immobilized *E.coli* on the tapered surface. Due to interaction between SNPs and bacteria, the cell wall membrane can be destroyed and as a result, bacterial sytoplasm leaks out into the sensor surrounding area [17-19]. This cause of the dielectric constant of the biological medium to change that is in turn changes RI around the fiber sensor.

4.3. Investigation the antibacterial effect of silver nanoparticles and gold nanoparticles

For experimental control, the antibacterial effect of SNPs was compared with gold nanoparticles (GNPs). For this purpose *E.coli* bacteria were cultured in GCM with 0 μg ml^{-1} and 20 μg ml^{-1} of GNPs and SNPs and then, the results were compared. As it is shown in Fig. 9a, the growth of bacteria in both culture medium containing GNPs at the concentration of 20 μg ml^{-1} is closely identical to the 0 μg ml^{-1} concentration of SNPs, confirming the absence of the antibacterial properties in GNPs. To better illustrate the lack of antibacterial properties of GNPs, a comparison between the SNPs concentration of 20 μg ml^{-1} and GNPs was carried out. The results which given in Fig. 9b show a bacterial cell growth in GCM containing GNPs with 2 h growth delay phase and growth rate 0.94 h^{-1}. However culture medium containing SNPs inhabited the bacteria cell with inhibition rate of -0.31 h^{-1} and 3 h delay phase of inhibition. Therefore GNPs showed no growth-inhibitory effect against *E.coli* in our experiment. These results are consistent with the earlier reports [8,16].

[Figure 9 should be inserted in here]

4.4. Possible mechanism for antibacterial action of silver nanoparticles

Even though several research have been done to understand the mechanism that SNPs interact with bacteria, this process has not yet been fully elucidated. Investigators suggested that SNP interact with *E.coli* and change the morphology of its membrane. Consequently, bacterial cell layer become incapable of correctly controlling transport through the plasma membrane, resulting into cell death [52,53]. Outer

membrane of *E.coli* bacteria are made from tightly packed lipopolysaccharid molecules and the overall charge of bacterial cells at biological pH values are negative. Therefore, the negative charges on the bacterial surface are because of the carboxylic and phosphonate groups in the outer membrane. The opposite charges between SNPs and bacterial cell wall cause their adhesion and bioactivity due to the electrodynamics forces [54,55]. Also, SNPs interacted with phosphate and sulfur structures that are part of the cell membrane phospholipids or proteins [56-58]. SNPs can penetrate into cell membrane and also damage other bacterial vital structures containing phosphorus and sulfur compounds such as proteins and DNA. These interactions cause DNA loss and disability of the DNA to replicate [59]. Moreover cellular proteins become inactive after interaction with SNPs [60]. Another reason is the release of silver ion from SNPs. SNPs and silver ions generate reactive oxygen species (ROS) [61]. Inactivation of the enzymes bacteria after treatment by SNPs can be considered is another cause of bacterial death [62-63]. The various observed and hypothesized interactions between SNP and bacteria cells are conceptually illustrated in Fig. 10.

[Figure 10 should be inserted in here]

In Fig. 11 scanning electron microscopy (SEM) microphotographs show that the SNPs anchor the cell at several sites and perforations makes in the membrane, which could result in cell lyses. As demonstrated by electron microscopy, interaction with SNPs resulted in perforations in the cell wall, contributing to the antibacterial effects of the SNPs. This outcome is in agreement with the finding of Kim and pal et al., who's investigated observe signification killing of micro organism using silver NPs [8,16].

[Figure 11 should be inserted in here]

5. Conclusion

An optical fiber biosensor based on a NATOF sensor was successfully demonstrated and used for the study of the SNP antibacterial effects on the *E.coli K-12* by culturing the organisms in liquid broth. The results were compared with colony counting method for cells that were grown on the same medium. We evaluated the influence of NBM and GCM on the antibacterial activity of SNPs. Changing RI around the tapered region with interaction of SNPs with immobilized bacteria on the optical fiber surface was used as the recognition principle for the detection. The inhibition rate of the bacterial growth in GCM increased from - 3.0×10^{-3} h^{-1} to - 1.98×10^{-2} h^{-1} as the concentration of SNPs increased from 0 to 50 μg ml^{-1}. Also, antibacterial activities of SNPs have been successfully detected and quantified 3–6 times faster than conventional bacteriological techniques. The new antibacterial activity measurement system presents numerous advantages such as small size, rapid, and label-free performance intended for small analyte volumes. The NATOF biosensors may provide robust sensor plarform toward our understandings of other mechanism of antibacterial activity of SNPs with biosystems and other interfacial phenomena at nanoscale.

References

[1] C.N. Lok, C.M. Ho, R. Chen, Q.Y. He, W.Y. Yu, H. Sun, P.K.H. Tam, J.F. Chiu, C. M. Che, Proteomic analysis of the mode of antibacterial action of silver nanoparticles, J. Proteome Res. 5(4) (2006) 916-24.

[2] J. R. Morones, J. L. Elechiguerra, A. Camacho, K. Holt, J. Kouri, J.T. Ramirez, M. J. Yacaman, The Bactericidal effect of silver nanoparticles, Nanotechnol. 16 (2005) 2346-53.

[3] U.K. Parashar, P.S. Saxena, A. Srivastava, Role of nanomaterials in biotechnology, Dig. J. Nanomater Bios. 3 (2008) 81-87

[4] S. Pal, Y.K. Tak, J.M. Song, Does the antibacterial activity of silver nanoparticles depend on the shape of the nanoparticle? A study of the gram-negative bacterium *Escherichia coli*, Appl. Environ. Microbiol. 73 (2007) 1712.

[5] M. Raffi, F. Hussain, T. M. Bhatti, J. I. Akhter, A. Hameed and M. M. Hasan, Antibacterial characterization of silver nanoparticles against *E.coli ATCC-15224*, J. Mater. Sci. Technol., 24 (2008) 192-196.

[6] I. Sondi, B. Salopek-Sondi, Silver nanoparticles as antimicrobial agent: a case study of *E. coli* as a model for gram-negative bacteria, J. Colloid Interface Sci. 275 (2004) 177-82.

[7] A. Panacek, R. Prucek, M. Kolar, R. Vecerova, L. Kvtek, R.N. Pizurova, V.K.Tatjana, R. Zboril, Silver colloid nanoparticles: synthesis, characterization, and their antimicrobial activity, J. Phys. Chem. B 110 (2005) 16248-53.

[8] J.S. Kim, E. Kuk, K.N. Yu, J.H. Kim, S.H. Park, H.J. Lee, S.H. Kim. Antibacterial effects of silver nanoparticles, Nanomedicine. 3 (2007) 95-101.

[9] C. Baker, A. Pradhan, L. Pakstis, D.J. Pochan, S.J. Shah, Synthesis and antibacterial properties of silver nanoparticles, J. Nanosci. Technol. 5 (2005) 244-9.

[10] Y. Li, P. Leung, L. Yao, Q. W. Song and E. Newton, Antimicrobial effect of surgical masks coated with functional mnanoparticles, J. Hosp. Infec 62 (2006) 58-63.

[11] K.N.J. Stevens, O. Crespo-Biel, E.E.M. van den Bosch, A. A. Dias,M. L. W. Knetsch, Y. B. J. Aldenhoff, F. H. van der Veen, J. G. Maessen,E. E. Stobberingh, L. H. Koole, The relationship between the antimicrobial effect of catheter coatings containing silver nanoparticles and the coagulation of contacting blood, Biomaterials 30 (2009) 3682–90.

[12] A. Oloffs, C. Crosse-Siestrup, S. Bisson, M. Rinck, R. Rudolvh, and U. Gross, Biocompatibility of silver-coated polyurethane catheters and silver-coated Dacron® material, Biomaterials 15 (1994) 753–758.

[13] M.L. Gulrajani, D. Gupta, S. Periyasamy, S.G. Muthu, Preparation and application of silver nanoparticles on silk for imparting antimicrobial properties, Appl. Polym. Sci.108 (2088) 614–623.

[14] S. Tarimala, N. Kothari, N. Abidi, E. Hequet, J. Fralick, L.L. Dai , New approach to antibacterial treatment of cotton fabric with silver nanoparticle-doped silica using sol-gel process, Appl. Polym. Sci. 101 (2006) 2938–2943.

[15] G. Zhao, S.E. Stevens, Multiple parameters for the comprehensive evaluation of the susceptibility of *Escherichia coli* to the silver ion, Biometals 11 (1998) 27 - 32.

[16] A. Dror-Ehre, H. Mamane, T. Belenkova, G. Markovich, A. Adin, Silver nanoparticle *E. coli* colloidal interaction in water and effect on *E. coli* survival, J. Colloid and Interface Sci. 339 (2009) 521–526.

[17] Y. Zhou, Y. Kong, S. Kundu, J.D. Cirillo and H. Liang, Antibacterial activities of gold and silver nanoparticles against *Escherichia coli* and bacillus Calmette-Guérin, J. Nanobiotechnol.10:19 (2012), doi: 10.1186/1477-3155-10-19.

[18] M.G. Guzmán, J. Dille, S. Godet, Synthesis of silver nanoparticles by chemical reduction method and their antibacterial activity, J. Chem. and Biomolecul. Eng. 2 (2009) 104-111.

[19] W. Zhang, A.G. Stack, Y. Chen, Interaction force measurement between *E.coli* cells and nanoparticles immobilized surfaces by using AFM, Colloid surface B, 82 (2011) 316-324.

[20] D.W. Kim, Y. Zhang, K.L. Cooper, and A.Wang, Fiber-optic interferometric immuno-sensor using long period grating, Electron. Lett. 42 (2006) 324–325.

[21] P. Caldas, P.A.S. Jorge, F.M. Araújo, L.A. Ferreira, M.B. Marques, G. Rego, and J.L. Santos, Fiber modal Michelson interferometers with coherence addressing and heterodyne interrogation, Opt. Eng. 47 (2008) Paper 044401.

[22] J.L. Tang, S.F. Cheng, W.T. Hsu, T.Y. Chiang, and L.K. Chau, Fiber-optic biochemical sensing with a colloidal gold-modified long period fiber grating, Sens. Actuators B, 119(1) (2006) l05–109.

[23] M.I. Zibaii, H. Latifi, K. Karami, M. Gholami, S.M. Hosseini, and M.H. Ghezelayagh, Non-adiabatic tapered optical fiber sensor for measuring the interaction between α-amino acids in aqueous carbohydrate solution, J. Meas. Sci. Technol. 21 (2010), Paper 105801.

[24] P. Zhua, D.R. Shelton, J.S. Karns, A. Sundaram, S. Li, P. Amstutz, C.M. Tang, Detection of water-borne *E. coli* O157 using the integrating waveguide biosensor, Biosens. Bioelectron. 21 (2005) 678–683.

[25] S.H. Ohk, Arun K. Bhunia, Multiplex fiber optic biosensor for detection of Listeria monocytogenes, *Escherichia coli O157:H7* and Salmonella enterica from ready-to-eat meat samples, Food Microbiol. 33 (2013) 166- 171.

[26] D.R. DeMarco, E.W. Saaski, D.A. McCrae, D.V. Lim, Rapid detection of *Escherichia coli* O157: H7 in ground beef using a fiber-optic biosensor, J. Food Protect. 62 (7) (1999) 711–716.

[27] T. Geng, J. Uknalis, S.I. Tu, A.K. Bhunia, Fiber-optic biosensor employing Alexa-Fluor conjugated antibody for detection of *Escherichia coli* O157: H7 from ground beef in four hours, Sensors 6 (8) (2006) 796– 807.

[28] K. Rijal, A. Leung, P. Mohana Shankar, R. Mutharasan, Detection of pathogen *Escherichia coli* O157:H7 AT 70 cells/mL using antibody-immobilized biconical tapered fiber sensors, Biosens. Bioelectron. 21 (2005) 871–880.

[29] D. Maraldo, P.M. Shankar, R. Mutharasan, Measuring bacterial growth by tapered fiber and changes in evanescent field, Biosens. Bioelectron. 21 (2006) 1339–44.

[30] M.I. Zibaii, A. Kazemi, H. Latifi, M. Karimi Azar, S.M. Hosseini, and M.H. Ghezelaiagh, Measuring bacterial growth by RI tapered fiber optic biosensor, Photochem. Photobio. B 101 (2010) 313–320.

[31] A.P. Ferreira, M.M. Werneck, R.M. Ribeiro, Development of an evanescent-field fiber optic sensor for *Escherichia coli* O157:H7, Biosens. Bioelectron. 16 (2001) 399–408.

[32] R. Bharadwaj, V.V.R. Sai, K. Thakare, A. Dhawangale, T. Kundu, S. Tituse, P.K. Vermae, S. Mukherji, Evanescent wave absorbance based fiber optic biosensor for label-free detection of *E. coli* at 280nm wavelength, Biosens. Bioelectron. 26 (2011) 3367–70.

[33] P.M. Fratamico, T.P. Strobaugh, M.B. Medina, A.G. Gehring, Detection of Escherichia coli O157:H7 using a surface plasmon resonance biosensor. Biotech. Tech. 12 (1998) 571– 76.

[34] A.D. Taylor, Q. Yu, S. Chen, J. Homola, S. Jiang, Comparison of *E. coli O157:H7* preparation methods used for detection with surface plasmon resonance sensor, Sens. Actuators B Chem. 107 (2005) 202-8.

[35] Y. Wang, Z. Ye, C. Si, Y. Ying, Monitoring of *Escherichia coli O157:H7* in food samples using lectin based surface plasmon resonance biosensor, Food Chem. 136 (2013) 1303–8.

[36] J. Waswa, J. Irudayaraj, C. DebRoy, Direct detection of *E. Coli O157:H7* in selected food systems by a surface plasmon resonance biosensor, LWT—Food Sci. Technol. 40 (2007) 187–192.

[37] N. Tawil, E. Sacher, R. Mandeville, M. Meunier, Surface plasmon resonance detection of *E. coli* and methicillin-resistant S. aureus using bacteriophages, Biosens. Bioelectron. 37 (2012) 24–29.

[38] Y. Wang, W. Knoll, and J. Dostalek, Bacterial pathogen surface plasmon resonance biosensor advanced by long range surface plasmons and magnetic nanoparticle assays, Anal. Chem. 84 (2012) 8345−50.

[39] A. Ramachandran, S. Wang, J. Clarke, S.J. Ja, D. Goad, L. Wald, E.M. Flood, E. Knobbe, J.V. Hryniewicz, S.T. Chu, D. Gill, W. Chen, O. King, B.E. Little, A universal biosensing platform based on optical micro-ring resonators, Biosens. Bioelectron. 23 (2008) 939-44.

[40] H.C. Ren, F. Vollmer, S. Arnold and A. Libchaber, High-Q microsphere biosensor - analysis for adsorption of rod like bacteria, Opt. Express15 (2007) 17410-23.

[41] M. Smietana, W.J. Bock, P. Mikulic, A. Ng, R. Chinnappan and M. Zourob, Detection of bacteria using bacteriophages as recognition elements immobilized on long-period fiber gratings, Opt. Express. 19 (2011) 7971-78.

[42] S.M. Tripathi, W.J. Bock, P. Mikulic, R. Chinnappan, A. Ng, M. Tolba, M. Zourob, Long period grating based biosensor for the detection of Escherichia coli bacteria, Biosens. Bioelectron. 35 (2012) 308– 312.

[43] A. Mazhorova, A. Markov, A. Ng, R. Chinnappan, O. Skorobogata, M. Zourob, and M. Skorobogatiy, Label-free bacteria detection using evanescent mode of a suspended core terahertz fiber, Opt. Express 20(5) (2011) 5344-55.

[44] K.Q. Kieu and M. Mansuripur, Biconical fiber taper sensor, IEEE Photon. Technol. Lett., 18(21) (2006) 2239–41.

[45] J.D. Love, W.M. Henry, W.J. Stewart, R.J. Black, S. Lacroix, and F. Gonthier, Tapered single-mode fibers and devices. Part I: adiabaticity criteria, IEE Proc. J. Optoelectron. 138 (1991) 343–54.

[46] P. Lu, L. Men, K. Sooley, and Q. Chen, Tapered fiber Mach– Zehnder interferometer for simultaneous measurement of refractive index and temperature, Appl. Phys. Lett. 94(2009) 131110.

[47] P. Lu, J. Harris, X. Wang, G. Lin, L. Chen, and X. Bao, Tapered-fiber-based refractive index sensorat an air/solution interface, Appl. Opt. 51(30) (2012) 7368-73.

[48] A. W. Snyder and J. D. Love, Optical Waveguide Theory, (Chapman and Hall, London, 1983).

[49] P. Polynkin, A. Polynkin, N. Peyghambarian, M. Mansuripur, Evanescent field-based optical fiber sensing device for measuring the refractive index of liquids in microfluidic channels, Opt. Lett. 30 (2005) 1273-75.

[50] F. Mirzajani, A. Ghassempour, A. Aliahmadi, M. A. Esmaeili, Antibacterial effect of silver nanoparticles on Staphylococcus aureus, Res. Microbiol. 162 (2011) 542-49.

[51] S. Shrivastava, T. Bera, A. Roy, G. Singh, P. Ramachandrarao and D. Dash, Characterization of enhanced antibacterial effects of novel silver nanoparticles, Nanotechnol.18 (2007) 225103 (9pp).

[52] C. Damm, H. Munstedt, Kinetic aspects of the silver ion release from antimicrobial polyamide/silver nanocomposites. Appl. Phys. A 91(2008) 479–86.

[53] A.L. Neal, What can be inferred from bacterium-nanoparticle interactions about the potential consequences of environmental exposure to nanoparticles?, Ecotoxicology 17 (2008) 362–71.

[54] O. Choi, K. Deng, N. Kim, L. Ross, R. Surampalli, Z. Hu, The inhibitory effects of silver nanoparticles, silver ions, and silver chloride colloids on microbial growth, Water Res 42 (2008) 3066–74.

[55] C. Marambio-Jones, E.M.V. Hoek, A review of the antibacterial effects of silver nanomaterials and potential implications for human health and the environment, J. Nanopart. Res. 12 (2010) 1531–51.

[56] P. Dibrov, J. Dzioba, K. Gosink, C. Hase, Chemiosmotic mechanism of antimicrobial activity of Ag+ in Vibrio cholerae. Antimicrob, Agents Chemother. 46 (2002) 2668–70.

[57] K. Holt, A. Bard, Interaction of silver (I) ions with the respiratory chain of Escherichia coli: an electrochemical and scanning electrochemical microscopy study of the antimicrobial mechanism of micromolar Ag, Biochem. 44 (2005) 13214–23.

[58] C. Lok, C. Ho, R. Chen, Q. He, W. Yu, H. Sun, P. Tam, J. Chiu, C. Che, Proteomic analysis of the mode of antibacterial action of silver nanoparticles. J. Proteome Res. 5 (2006) 916–24.

[59] Q. L. Feng, J. Wu, G. Q. Chen, F. Z. Cui, T. M. Kim, and J. O. Kim, A mechanistic study of the antibacterial effect of silver ions on *Escherichia coli* and *Staphylococcus aureus*. J. Biomed. Mater. Res. 52 (2000) 662–668.

[60] M. Yamanaka, K. Hara, and J. Kudo, Bactericidal actions of a silver ion solution on Escherichia coli, studied by energy-filtering transmission electron microscopy and proteomic analysis, Appl. Environ. Microbiol. 71 (2005) 7589–7593.

[61] T. Xia, M. Kovochich, J. Brant, M. Hotze, J. Sempf, T. Oberley, C. Sioutas, J.I. Yeh, M.R. Wiesner, A.E. Nel, Comparison of the abilities of ambient and manufactured nanoparticles to induce cellular toxicity according to an oxidative stress paradigm. Nano Lett. 6 (2006) 1794–1807.

[62] O. Choi, Z. Hu, Size dependent and reactive oxygen species related nanosilver toxicity to nitrifying bacteria, Environ. Sci. Technol. 42 (2008) 4583–88.

[63] S. J. Stohs, D. Bagchi, Oxidative mechanisms in the toxicity of metal-ions, Free Radic. Biol. Med. 18 (1995) 321–336.

Figure legend

Fig.1. (a) Schematic representation of NATOF, (b) conceptual representation as a modal Mach–Zehnder interferometer.

Fig. 2. Schematic of experimental setup for measuring the inhibition rate of the bacteria growth by NATOF sensor

Fig. 3. SEM microphotographs showing of (a) a section of waist of tapered fiber, and (b) one conic section of the NATOF

Fig. 4. Bacteria that are grown on agar plates at 0 μg ml^{-1}, 10 μg ml^{-1} and 30 μg ml^{-1} of SNPs in (a) NBM, and (b) GCM. Right plate is agar without SNPs as a control plate.

Fig. 5. Plot of *E. coli* concentration as a function of time for (a) NBM, and (b) GCM. Sample taken every 1h were counted by pour plate method and growth mediums containing different concentrations of SNPs.

Fig. 6. Effect of SNP concentrations on (a) bacterial growth rate constant (μ) and (b) the initial cell count (Ln N_0). Culture was grown on the GCM growth medium containing different concentrations of SNPs.

Fig. 7. Spectral response of the NATOF for before and after cell immobilization on the optical fiber biosensor

Fig. 8. (a) Bacterial dynamic growth curve in GCM during immobilized *E. coli* on the tapered fiber surface interacted with different concentration of SNP in GCM solution, and (b) Plot of sensor response versus time during 0.2 h-1.2 h.

Fig. 9. Bacterial growth dynamic curve in GCM after sedimentation and resuspension of the bacteria at (a) 0 μg ml^{-1} and 20 μg ml^{-1} of GNP, and (b) 20 μg ml^{-1} of GNP and SNP which are obtained by colony counting method.

Fig. 10. Diagram summarizing the interaction SNPs with bacterial cells. SNPs may (I) change membrane morphology and the bacterial cells incapable of correctly controlling transport through the plasma membrane; (II) interact with membrane proteins affecting their correct function; (III) enter into the cell where it can generate ROS, release silver ions, and affect DNA and inactivate of the enzymes bacteria.

Fig. 11: SEM microphotographs showing of (a) immobilized cells on the tapered fiber, and (b) interaction of SNPs with *E.coli* which are shown in side of ellipsoid. Some salt crystals are formed around the SNP because the PBS-A solution is evaporating.

Table legend

Table1. Comparison of various methods for investigation the interaction between bacteria and SNPs

Table 2. Optical biosensors for *E.coli* detection

Table3. Constant parameters of inhibition growth rate equation (Eq. 4).

Table 4. The inhibition rate of bacterial growth constant in colony counting method and specific inhibition growth rate in fiber sensor

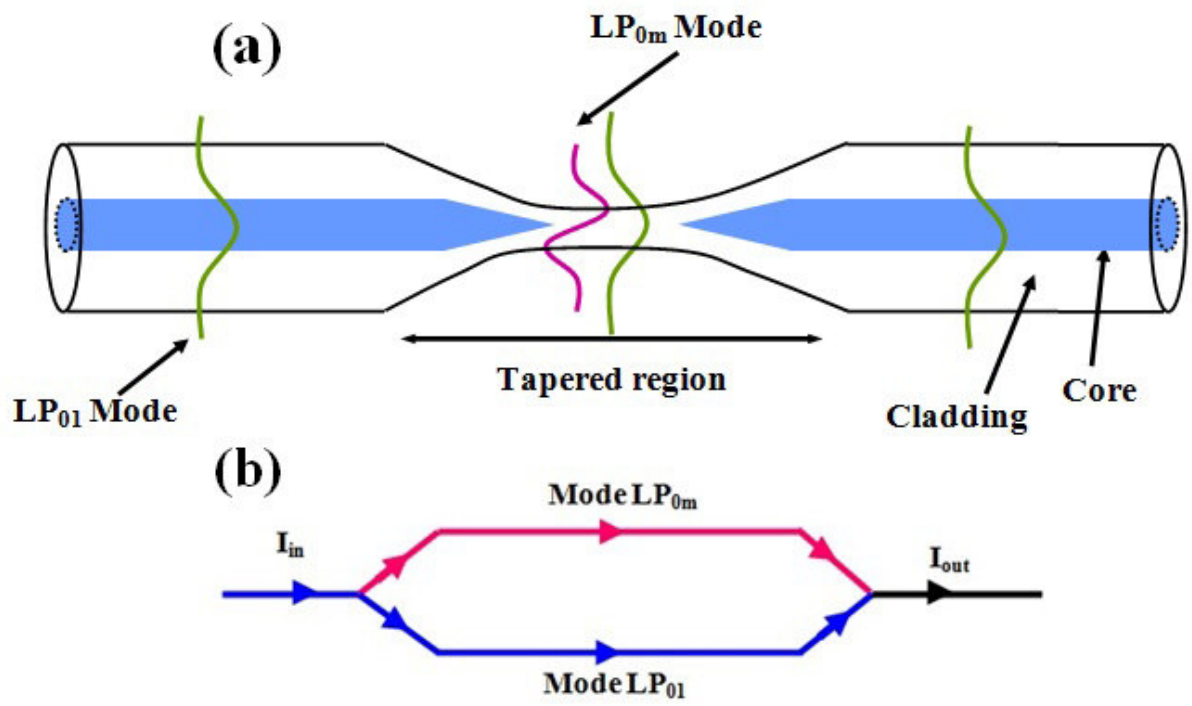

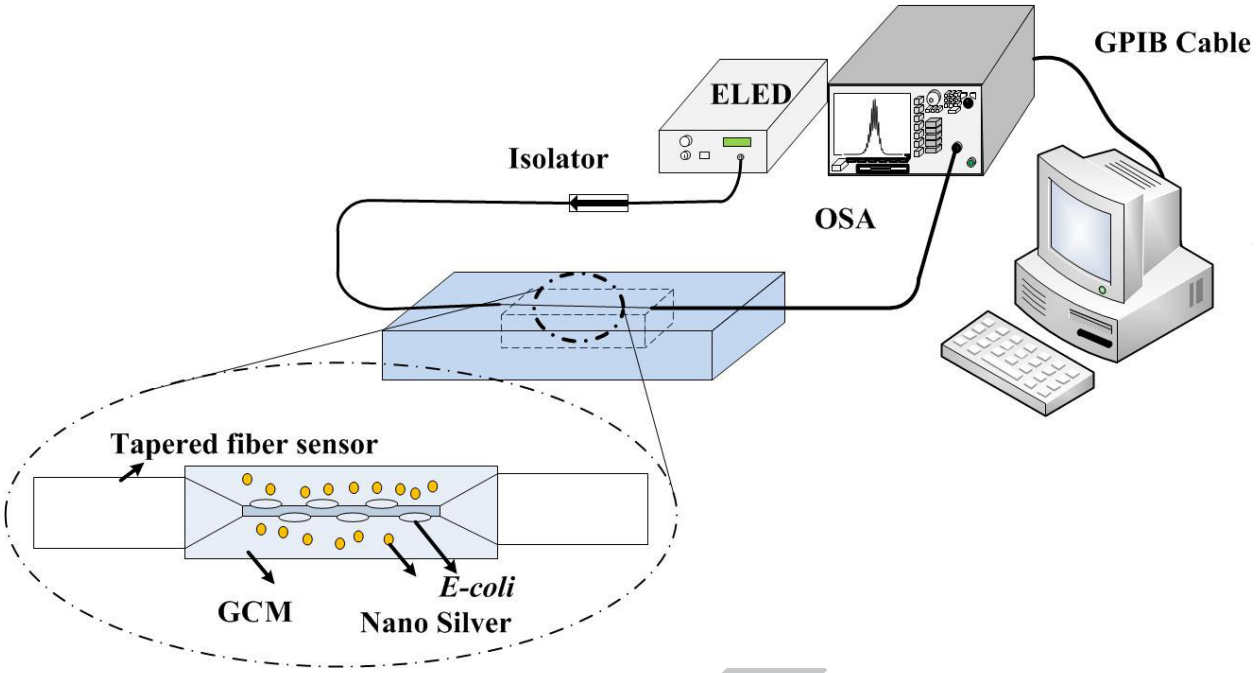

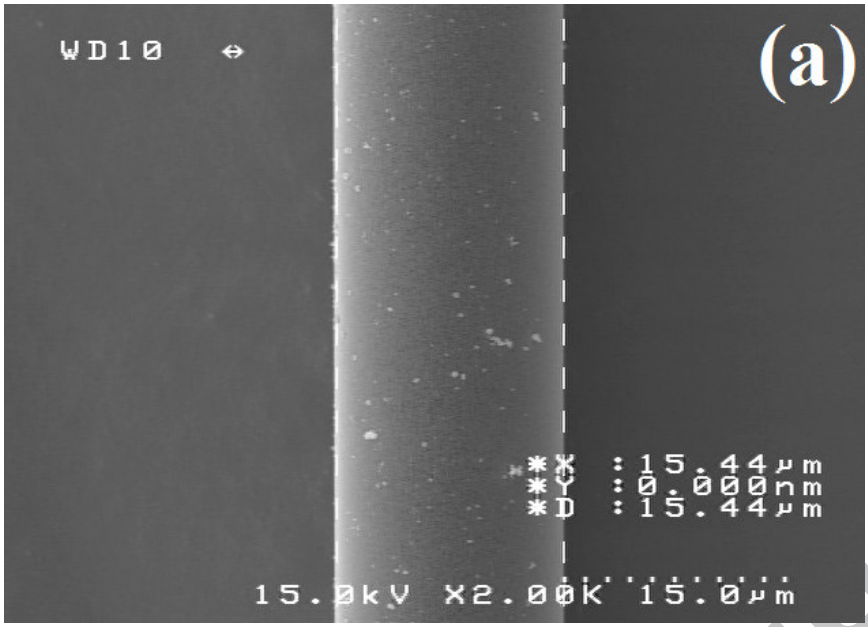

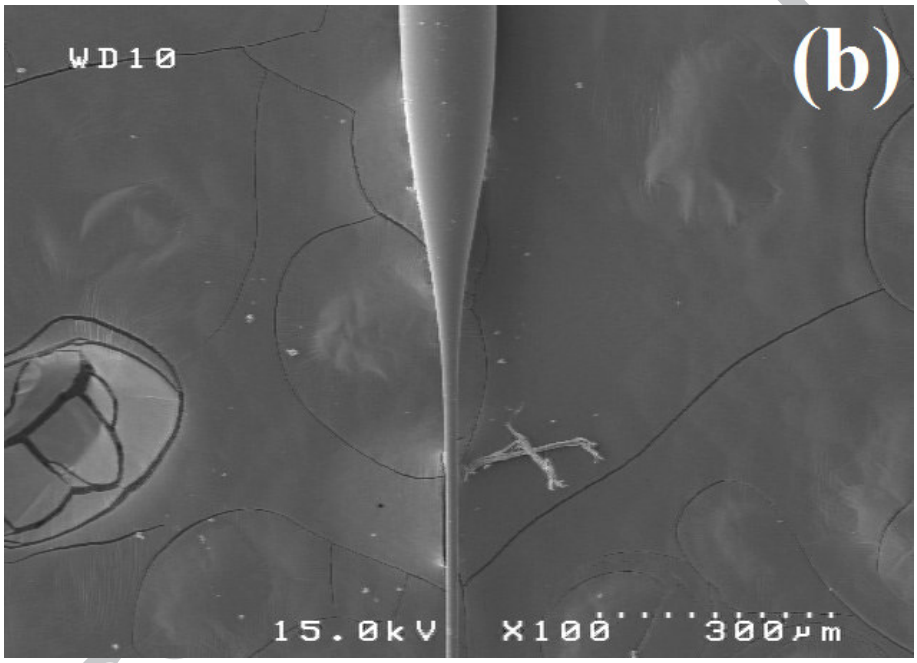

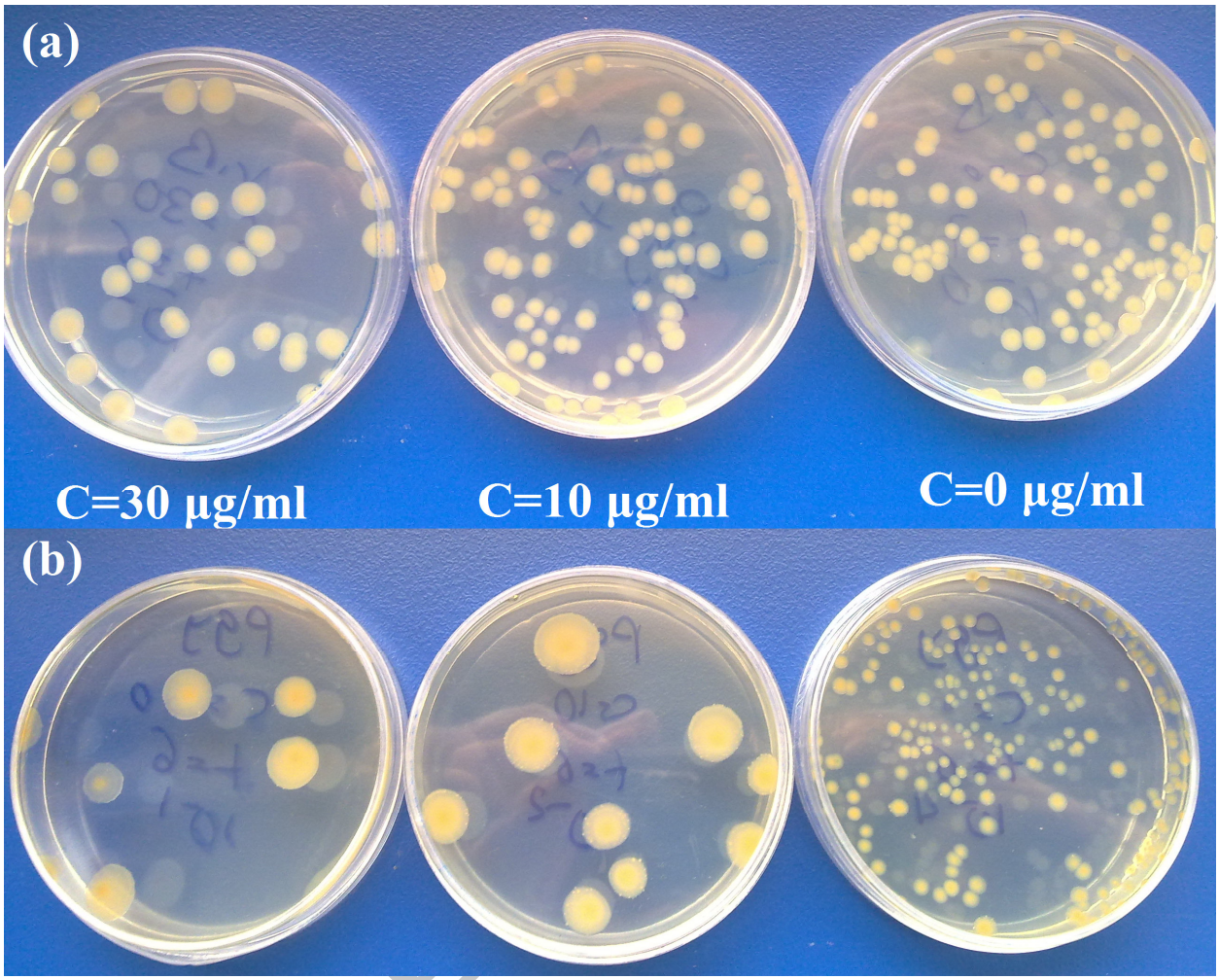

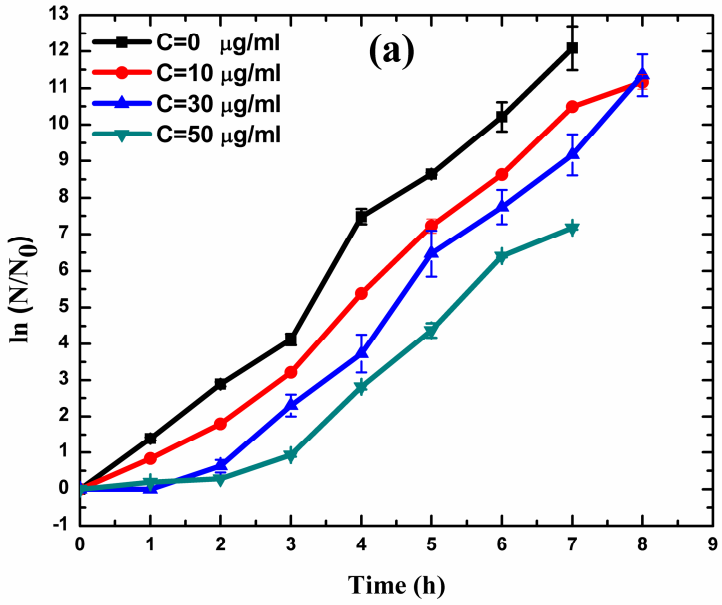

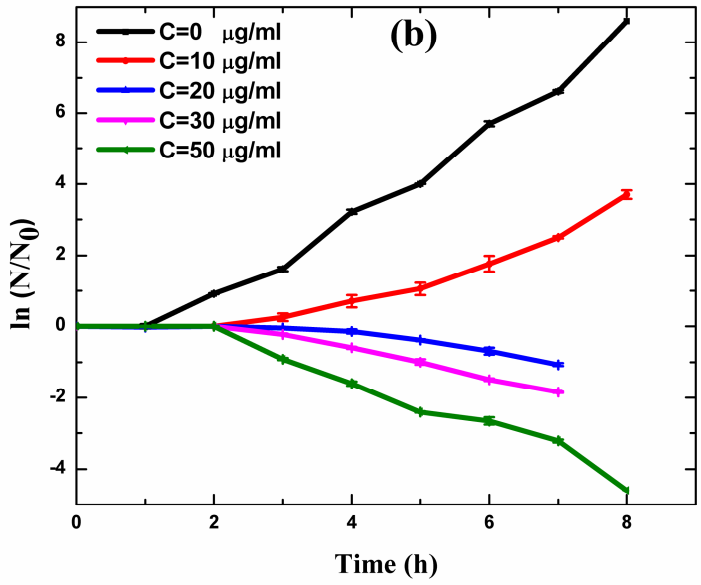

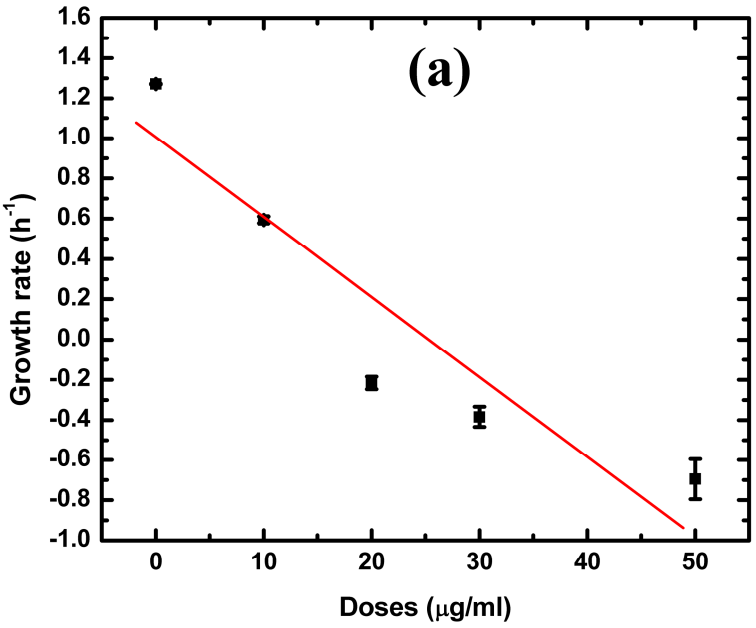
(a)
Growth rate (h-1)
1.6
1.4
1.2
1.0
0.8
0.6
0.4
0.2
0.0
-0.2
-0.4
-0.6
-0.8
-1.0
0
10
20
30
40
50
Doses (μg/ml)

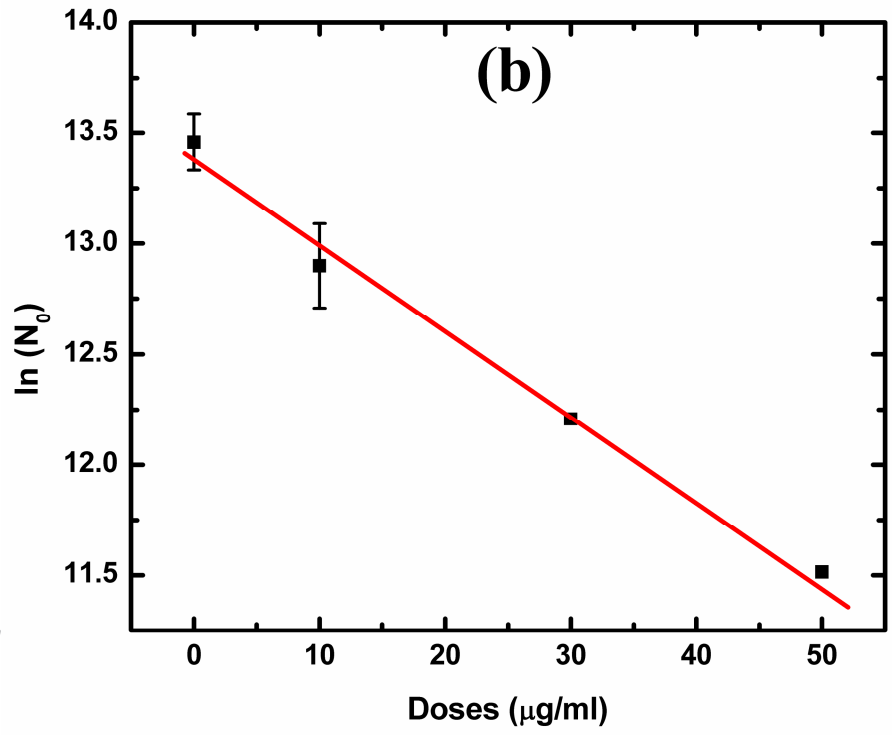
(b)
ln (N0)
14.0
13.5
13.0
12.5
12.0
11.5
0
10
20
30
40
50
Doses (μg/ml)

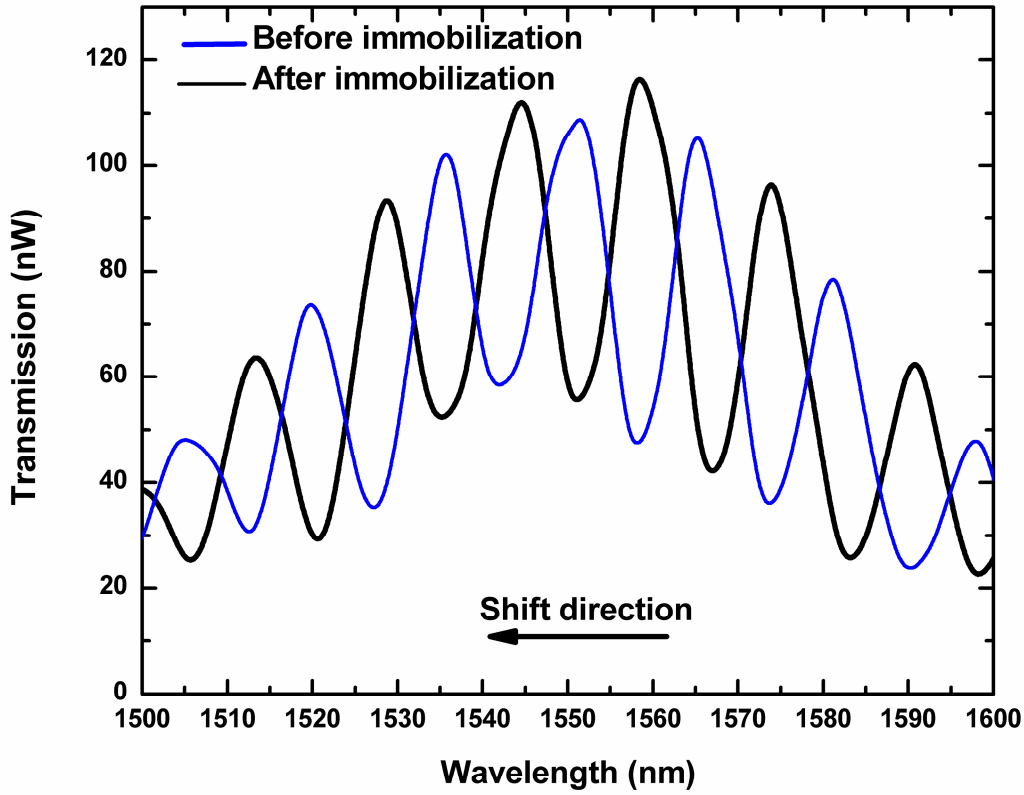

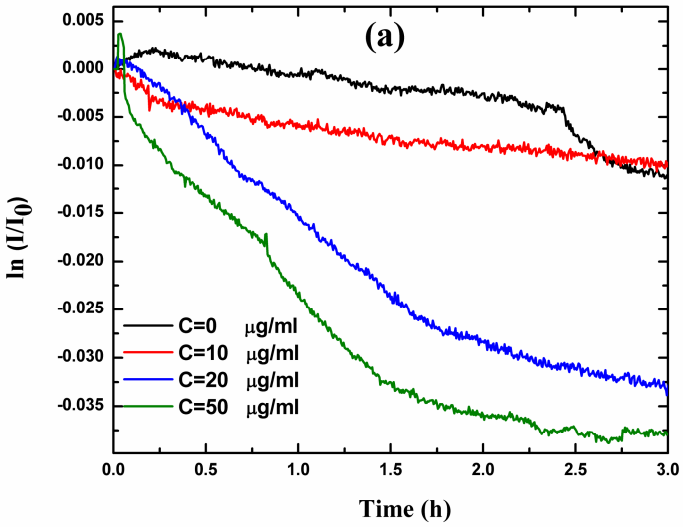

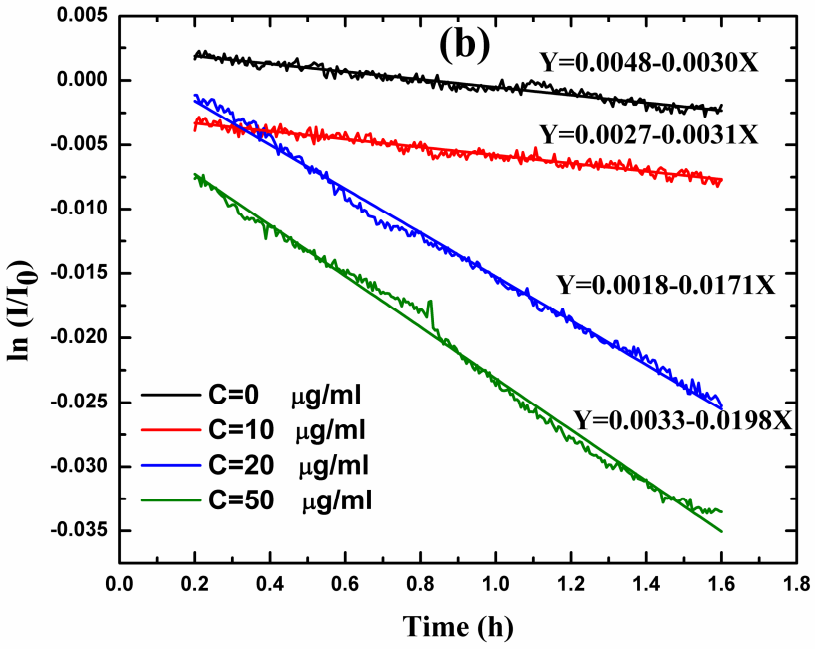

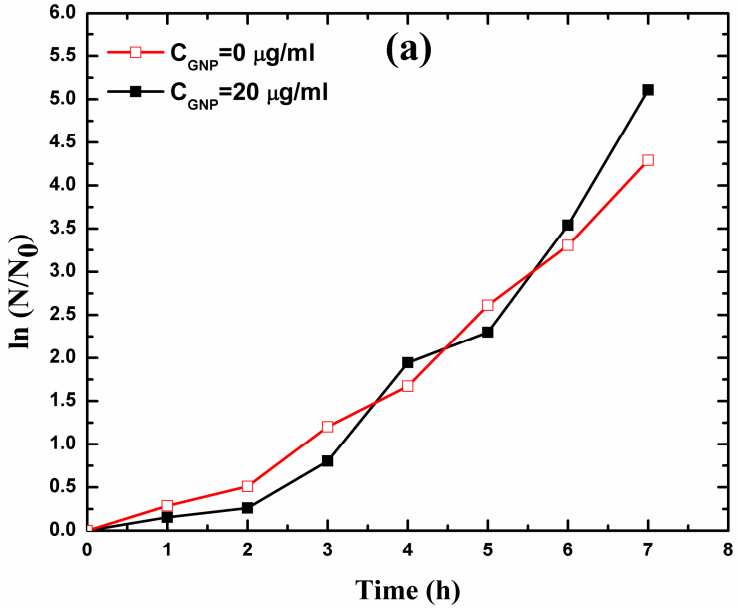

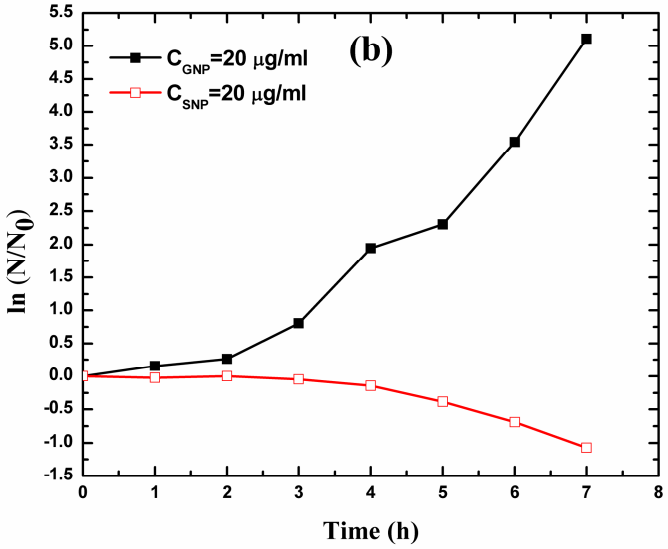

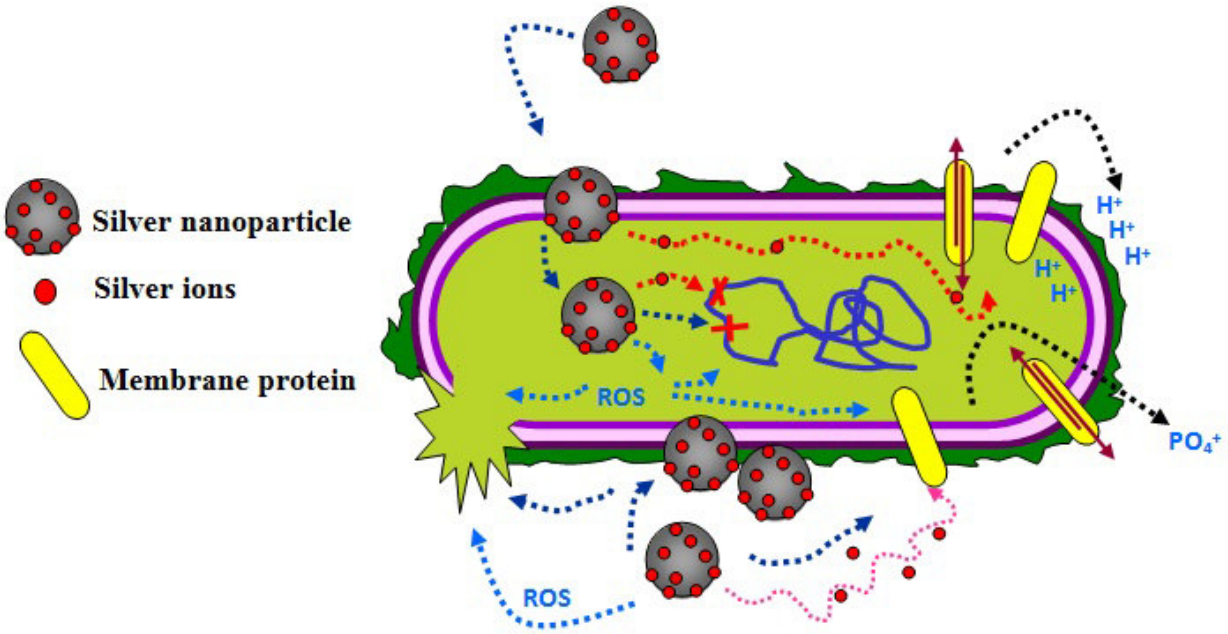

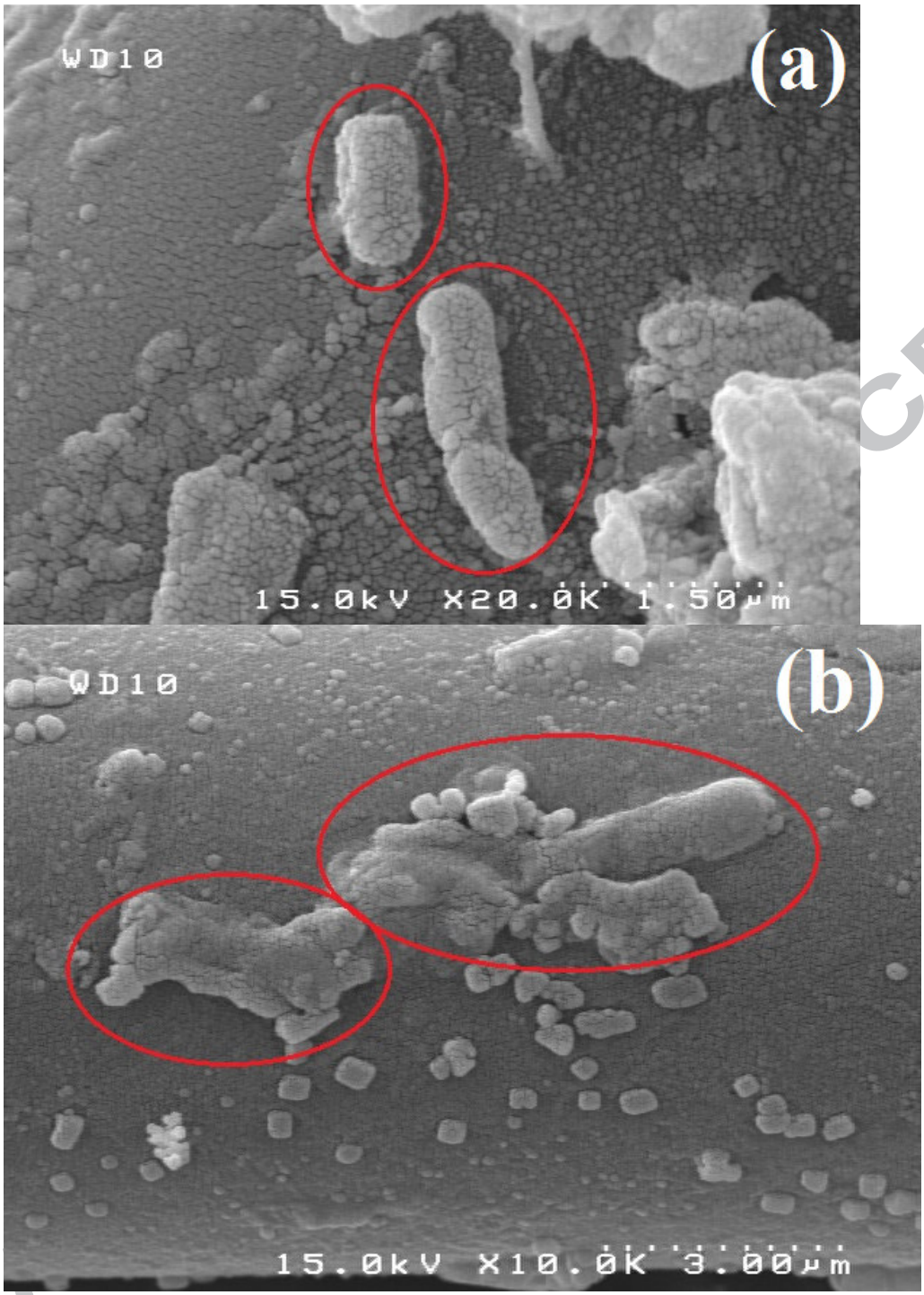
WD10
(a)
15.0kV X20.0K 1.50µm
WD10
(b)
15.0kV X10.0K 3.00µm

Method	Medium	Bacteria	MIC(μg ml^{-1})	Key accepts	[Ref]
Optical density measurement(OD)	liquid	Gram negative(10^4)	20-60	-Measured periodically up to 24 hours -With increasing concentration of SNP the OD decreased.	[16]
Estimation of colony forming units (CFU)	solid	Gram negative(10^4)	20-60	-Error in counting -The number of CFU have reduced with increasing SNP	[17]
SEM analysis of particles-bacteria interaction	solid	Gram negative(10^4)	Control method	-Observation of SNP adhered to the membrane of bacteria -Determined the distribution and location of SNP	[6]
TEM analysis of particles-bacteria interaction	solid	Gram negative(10^4)	Control method	-Observation of SNP adhered at the surface of the cell membrane penetrated inside the bacterial cell -Determined the distribution and location of SNP	[2,6]
X-ray energy dispersive spectrometry (XEDS)	solid	-	Control method	-Analysis of the organic-inorganic hybrid	[2,6]
Kirby-Bauer diffusion	solid	10^5 to 10^6 CFU ml^{-1}	6.74	-Determine the resistance or sensitivity of an organism to different antibiotics	[18]
Atomic force microscopy	aqueous	-	Control method	-Force measurement between *E.coli* and NPs immobilized on cantilever surface -The size dependent of adhesion force between *E.coli* cells and NPs of Different sizes may arise from the effective contact area	[19]

Technology platform	Optical structures	*E. coli* strain	LOD	Detection principle	Ref.
waveguide	glass capillary	*E.coli O157:H7.*	10 cells per capillary (0.075 ml volume)	fluorescent sandwich assay	[24]
	polystyrene waveguide	*E.coli O157:H7*	10^3 CFU ml^{-1}	Fluorescent sandwich assay	[25]
	Uniform MM polystyrene	**E.coli O157:H7.*	1 CFU ml^{-1}	Fluorescent sandwich assay	[26,27]
Tapered fiber	Single mode Biconical taper	*E. coli* O157:H7	70 Cells/mL	Absorption	[28]
	Single mode Biconical taper	*E. coli* JM 101	ND	Absorption	[29]
	Nonadiabatic	*E.coli K12*	60 *E. coli* /mm^2	RI	[30]
Chemical etched optical fibre	graded-index multimode	*E.coli O157:H7.*	10-800 Cell	Absorption	[31]
U-bent optical fiber	declladded fiber	*ND*	1000 CFU ml^{-1}	Absorption	[32]
Surface Plasmon Resonance (SPR)	Prism-based SPR	E. coli O157:H7	5×10^7 CFU ml^{-1}, 10^6 CFU ml^{-1} 3×10^3 CFU ml^{-1} 10^2–10^3 CFU ml^{-1} 10^3 CFU ml^{-1}	RI	[33,34] [35] [36] [37]
	SPR with magnetic nanoparticle assays	*E.coli O157:H7.*	50 CFU ml^{-1},		[38]
micro-optical resonators	Ring on a chip Dielectric		10^5 CFU ml^{-1}		[39]
	Fiber optic Microsphere	*E.coli K12*	10^2 Bacteria mm^{-2}	RI	[40]
	Long period fiber grating	*E. coli K12*	10^3 CFU ml^{-1}	RI	[41,42]
THz fiber	suspended core	*E. coli* B	10^4 CFU ml^{-1}	absorption	[43]

* In ground beef samples, Abbreviations: ND= not described

bacteria	a (ml μg^{-1} s^{-1})	b (s^{-1})	c (ml μg^{-1})	d
E.coli	0.024	1.232	0.038	-13.372

Concentration ($\mu g\ ml^{-1}$)	Method	
	Colony counting[1] $\mu(h^{-1})$	Fiber sensor[2] $\beta\mu$
0	1.270	-3.00×10^{-3}
10	0.594	-3.12×10^{-3}
20	-0.216	-1.71×10^{-2}
50	-0.694	-1.98×10^{-2}

[1] in duratuion 2 h to 5 h, [2]in duration 0.2 h 1.6 h

Highlights

- Fabricate a label free optical fiber biosensor for monitoring antibacterial activity of silver nanoparticle(SNP).
- Rapid analysis compared to conventional bacteriological techniques.
- We examine the influence of the bacterial media on the antibacterial effectiveness of the SNPs.
- We measure inhibition bacterial growth rate with colony counting and fiber optic biosensor.
- We report a novel sensing method for study mechanism of antibacterial activity of SNPs with biosystems